Near-Capacity Network Coding for Cooperative Multi-User Communications

Hung Viet Nguyen[1], Soon Xin Ng[1], João Luiz Rebelatto[2], Yonghui Li[3] and Lajos Hanzo[1]
[1]School of Electronics and Computer Science, University of Southampton, SO17 1BJ, United Kingdom.
[2] Dept. of Electrical Engineering, Federal University of Santa Catarina, Florianópolis, SC, 88040-900, Brazil.
[3]School of Electrical & Information Engineering, University of Sydney, Sydney, NSW, 2006, Australia.
Emails: [1]{hvn08r,sxn,lh}@ecs.soton.ac.uk; [2]jlrebelatto@eel.ufsc.br; [3]lyh@ee.usyd.edu.au

Abstract— **In this contribution, we investigate Near-Capacity Multi-user Network-coding (NCMN) based systems using an Irregular Convolutional Code, a Unity-Rate Code and M-ary Phase-Shift Keying. In the NCMN based systems, we consider a multiuser network in which the users cooperatively transmit independent information to a common base station (BS). Extrinsic Information Transfer (EXIT) charts were used for designing the proposed NCMN scheme. The design principles presented in this contribution can be extended to a vast range of NCMN based systems using arbitrary channel coding schemes.**

I. Introduction

Network coding is a recently introduced paradigm conceived for efficiently disseminating data in multicast wireless networks, where the data flows arriving from multiple sources are combined to achieve compression and hence to increase the achievable throughput, as well as to reduce the delay imposed and to enhance the error-resilience [1]–[3]. The relay nodes store the incoming packets in their own buffer and then transmit the linear combinations of these packets. The coefficients used for creating the linear combination may be random numbers defined over a large finite field [4], or those gleaned from parity-check matrices of error control codes [5], [6].

Generalised Dynamic Network Codes (GDNC) were proposed in [6], [7] by interpreting the design problem of network code as being equivalent to that of designing linear block codes defined over GF(q) for erasure correction. The authors of [6], [7] extended the original Diversity Network Code (DNC) concept presented in [8], which had been named Dynamic Network Code in [9], by allowing each user to broadcast several (as opposed to a single in [8], [9]) information frames (IFs) of its own during the broadcast phase via orthogonal channels. Similarly, during the cooperative phases, each user transmits an arbitrary number of nonbinary linear combinations to the base station (BS) using orthogonal channels, and these nonbinary linear combinations are considered as parity frames (PFs). In [6], [7], the authors investigated GDNCs assuming an idealised or so-called 'perfect' channel coding scheme, which was defined as the code that is capable of operating right at the Continuous-input Continuous-output Memoryless Channel's (CCMC) capacity. The Frame Error Ratio (FER) performance of the GDNC scheme was determined in [6] by calculating the rank of the matrix characterising GDNCs. This method, which we refer to as the Purely Rank-Based Method (PRBM), always provides an optimistic estimate of the attainable FER performance of GDNCs.

Tüchler and Hagenauer proposed the employment of Irregular Convolutional Codes (IrCCs) [10], [11] for serially concatenated schemes, which are constituted by a family of convolutional codes having different rates, in order to design a near-capacity system. They were specifically designed with the aid of Extrinsic Information Transfer (EXIT) charts conceived for analysing the convergence properties of iterative decoding aided concatenated coding schemes [12].

The financial support of the Vietnamese International Education Development (VIED) fund and the EU under the auspices of the OPTIMIX project as well as of the RC-UK under the India-UK Advanced Technology Centre is gratefully acknowledged.

As a further advance, it was shown in [13] that a recursive Unity-Rate Code (URC) having an infinite impulse response is capable of efficiently spreading the available extrinsic information across the entire iterative receiver chain. This URC may be employed as an intermediate code, in order to improve the attainable decoding convergence. The URC may be viewed as a precoder invoked for creating a serially concatenated inner code component having an infinite impulse response in order to reach the (1,1) point in the EXIT chart and hence to achieve an infinitesimally low Bit Error Ratio (BER) [14], as detailed in [15]. For example, a near-capacity Irregular Convolutional Coded (IrCC)-URC-M-ary Phase-Shift Keying (IrCC-URC-MPSK) scheme may be designed for the sake of approaching the achievable channel capacity.

Based on this background, *the novel contribution of this paper is that a realistic near-capacity channel coding scheme is designed for the sake of supporting network-coding aided multi-user communications. We consider the effects of both the shadow fading and of the small-scale Rayleigh fading in our channel model. The performance of the proposed system obtained by simulations is compared to that estimated by PRBM*. The specific design guidelines presented in this contribution can also be extended to a diverse range of network-coding aided multi-user systems employing arbitrary channel coding schemes.

The rest of this paper is organised as follows. In Section II, outage probabilities are derived, before detailing both our system model and the detector used at the BS. In Section III, we propose design procedures for both our near-capacity IrCC-URC-MPSK and for network coding models. Our performance results are presented and discussed in Section IV, before concluding the paper in Section V.

II. Preliminaries

A. Single Link Channel Outage Probability

We consider a single transmission link associated with the transmitted and received signals of x and y, respectively. The received signal can be represented as

$$y = hx + n \ , \tag{1}$$

where $h = h_s h_f$ is the complex-valued fading coefficient that comprises two components, a slow fading coefficient (large-scale shadow fading or quasi-static fading) h_s, which is constant for all symbols within a frame and a fast fading (small-scale Rayleigh fading) coefficient h_f, which varies on a symbol by symbol basis, while n is the Additive White Gaussian Noise (AWGN) process having a variance of $N_0/2$ per dimension.

We refer to C as the maximum achievable transmission rate of reliable communication supported by this channel. Let us assume that the transmitter encodes data at a rate of R bits/s/Hz. If the channel realisation h has a capacity of $C|_h < R$, the system is declared to be in outage, where the outage probability is given by:

$$P_e(R) = Pr\left\{C|_h < R\right\} \ , \tag{2}$$

978-1-4244-8325-9/11/$26.00 ©2011 IEEE

and $C|_h$ is the capacity, i.e. the maximum achievable rate of the channel, provided that h is known. If x is i.i.d., the transmission link obeys the CCMC model. The outage probability for the CCMC channel is given by [16]

$$P_e^{CCMC}(R) \quad = \quad Pr\left\{|h_s|^2 \mathrm{E}\left[|h_f|^2\right] < \frac{2^R-1}{SNR}\right\} \ , \qquad (3)$$

where SNR is the signal to noise power ratio. Furthermore, the maximum achievable transmission rate of reliable communication supported by the Discrete-input Continuous-output Memoryless Channel (DCMC) was shown to be [17]

$$C^{DCMC}(\eta) = \eta - \frac{1}{2^\eta}\sum_{l=1}^{L} E\left[\log_2 \sum_{z=1}^{L} \exp(\psi_{l,z})\bigg|_{X_l}\right], \qquad (4)$$

where $L = 2^\eta$ is the number of modulation levels, while η is the number of modulated bits, and $E[A|X_l]$ is the expectation of A conditioned on the L-ary signals X_l, whereas $\psi_{l,z}$ is defined in [17].

We define the receiver's SNR as $SNR_r = E[|h|^2 SNR]$. At a given data rate $R = \eta R_c$, where R_c is the channel coding rate, we readily identify the corresponding $SNR_r|_R$ on the DCMC capacity curve described by (4). Then, similar to (3), the outage probability of the DCMC model is equivalent to the probability of the specific event that we have $|h|^2 SNR < SNR_r|_R$:

$$P_e^{DCMC}(R,\eta) = Pr\left\{|h_s|^2 \mathrm{E}[|h_f|^2] < \frac{SNR_r|_R}{SNR}\right\}. \qquad (5)$$

B. System Model

Let us initially describe a simple system having $M = 2$ users communicating with a BS [9]. A transmission session consists of $(k_1M + k_2M) = 4$ phases that include broadcast phases B_1 and B_2 and cooperative phases C_1 and C_2. In the transmission session, each user transmits $k_1 = 1$ IF during the corresponding broadcast phase and $k_2 = 1$ PF during the corresponding cooperative phase according to the transfer matrix $\boldsymbol{G}_{2\times4}$ [8], [9]:

$$\boldsymbol{G}_{2\times4} = \left[\begin{array}{cc|cc} 1 & 0 & 1 & 1 \\ 0 & 1 & 1 & 2 \end{array}\right], \qquad (6)$$

where the PF transmitted by User 1 (or User 2) during the cooperative phase C_1 (or C_2) is given by PF=$\boldsymbol{G}_{2\times4}(1,3)I_1(1) + \boldsymbol{G}_{2\times4}(2,3)I_2(2) = I_1(1) + I_2(2)$ (or PF=$\boldsymbol{G}_{2\times4}(1,4)I_1(1) + \boldsymbol{G}_{2\times4}(2,4)I_2(2) = I_1(1) + 2I_2(2)$). The variable $I_i(i)$, $i = [1,2]$, represents the IF transmitted by User i during the broadcast phase B_i. In [6], [7], each user is allowed to broadcast an arbitrary number of k_1 IFs during the broadcast phase as well as to transmit an also arbitrary number of k_2 PFs in the cooperative phase. For simplicity, we refer to a single transmission phase (broadcast phase or cooperative phase) as a time slot (TS), in which a user transmits a single frame (IF or PF).

To elaborate further, let us define $\boldsymbol{G}'_{2\times4}$ as the corresponding *modified* transfer matrix, where the terminology *modified* implies that the entries of $\boldsymbol{G}'_{2\times4}$ are modified with respect to those of the original transfer matrix $\boldsymbol{G}_{2\times4}$ of (6) according to the success/failure of each transmission within the actual transmission session. If all the frames transmitted within the session are successfully decoded, the transmission session can be equivalently represented by the modified transfer matrix $\boldsymbol{G}'_{2\times4} = \boldsymbol{G}_{2\times4}$, where $\boldsymbol{G}'_{2\times4}(i,i) = \boldsymbol{G}_{2\times4}(i,i), i = [1,2]$ represents the successful decoding of the IF $I_i(i)$ at the BS. Note that having $\boldsymbol{G}'_{2\times4}(1,3) = \boldsymbol{G}_{2\times4}(1,3)$ (or $\boldsymbol{G}'_{2\times4}(2,4) = \boldsymbol{G}_{2\times4}(2,4)$) means that the PF transmitted by User 1 (or User 2) was successfully decoded at the BS. Similarly, having $\boldsymbol{G}'_{2\times4}(2,3) = \boldsymbol{G}_{2\times4}(2,3)$ (or $\boldsymbol{G}'_{2\times4}(1,4) = \boldsymbol{G}_{2\times4}(1,4)$) indicates that the IF $I_2(2)$ (or $I_1(1)$) was successfully decoded by User 1 (or User 2), and that the PF transmitted by User 1 (or User 2) was successfully decoded at the BS.

Let us consider the following example of the actual transmission session, where $'\rightarrow'$ represents the transmission direction, while $'=1'$ (or $'=0'$) above the arrows means that the frame was successfully (or unsuccessfully) recovered at the destination:

$$\begin{array}{ll} B_1 & \boldsymbol{G}'_{2\times4}(1,3) = \boldsymbol{G}_{2\times4}(1,3), \\ & [\text{User 1} \xrightarrow{=0} BS] : \boldsymbol{G}'(1,1) = 0, \\ & [\text{User 1} \xrightarrow{=1} \text{User 2}] : \boldsymbol{G}'_{2\times4}(1,4) = \boldsymbol{G}_{2\times4}(1,4), \\ B_2 & \boldsymbol{G}'_{2\times4}(2,4) = \boldsymbol{G}_{2\times4}(2,4), \\ & [\text{User 2} \xrightarrow{=0} BS] : \boldsymbol{G}'(2,2) = 0, \\ & [\text{User 2} \xrightarrow{=1} \text{User 1}] : \boldsymbol{G}'_{2\times4}(2,3) = \boldsymbol{G}_{2\times4}(2,3), \\ C_1 & [\text{User 1} \xrightarrow{=0} BS] : \boldsymbol{G}'_{2\times4}(i,3) = 0, i = 1,2, \\ C_2 & [\text{User 2} \xrightarrow{=1} BS] : \boldsymbol{G}'_{2\times4}(i,4) \text{ unchanged}, i = 1,2. \end{array} \qquad (7)$$

This example results in

$$\boldsymbol{G}'_{2\times4} = \left[\begin{array}{cc|cc} 0 & 0 & 0 & 1 \\ 0 & 0 & 0 & 2 \end{array}\right], \qquad (8)$$

where the diagonal elements "1" at the left of (6) become "0" owing to the unsuccessful [User 1 $\xrightarrow{=0} BS$] and [User 2 $\xrightarrow{=0} BS$] transmissions during the broadcast phases B_1 and B_2, respectively. The "0" elements in the third column of (8) indicate the unsuccessful [User 1 $\xrightarrow{=0} BS$] transmission during the cooperative phase C_1.

Let us now generalise this model. The transfer matrix $\boldsymbol{G}_{k_1M\times k_1M+k_2M}$ (or $\boldsymbol{G}$ for shorthand) seen in Fig. 1, which comprises the identity matrix $\boldsymbol{I}_{k_1M\times k_1M}$ (or $\boldsymbol{I}$ for shorthand) and the parity matrix $\boldsymbol{P}_{k_1M\times k_2M}$ (or $\boldsymbol{P}$ for shorthand) represents a ideal transmission session of the system, where all the frames transmitted during that session are successfully decoded. The binary flag $I_m^{Co}(t)$ seen in Fig. 1 represents the success or failure of the IF decoding at the BS, namely the IF $I_m(t), t = [m, M+m, ..., (k_1-1)M+m]$, transmitted by User m, $m \in \{1, ..., M\}$. Accordingly, we always have $I_m^{Co}(t) = 1$. The corresponding entry $I_m^{Co'}(t)$ is set during the specific broadcast phase t selected from the whole set of k_1M broadcast phases according to [6], [7]:

$$I_m^{Co'}(t) = \left\{\begin{array}{ccl} I_m^{Co}(t) & : & \text{If } I_m(t) \text{ is successfully recovered} \\ 0 & : & \text{Otherwise} \end{array}\right. . \qquad (9)$$

The k_2 PFs transmitted by each of the M users contain nonbinary linear combinations of its own IFs with the successfully decoded IFs from the set of $k_1(M-1)$ IFs transmitted by the $(M-1)$ other users. The variable $P_{m,s}(t)$ in Fig. 1 corresponds to the parity coefficient of the IF $I_r(t)$ contained in the s^{th} PF transmitted by User m during the cooperative phase $[M(s-1)+m]$, $s \in \{1, ..., k_2\}$, where we have the index r determined by

$$r = \left\{\begin{array}{ccl} M & : & t \bmod M = 0 \\ t \bmod M & : & t \bmod M \neq 0 \end{array}\right. . \qquad (10)$$

Let us denote the corresponding entry of $P_{m,s}(t)$ in the modified matrix $\boldsymbol{G}'$ as $P'_{m,s}(t)$, which is determined by

$$P'_{m,s}(t) = \{\ P_{m,s}(t) \ : \ r = m \ . \qquad (11)$$

Then, for the case that we have $r \neq m$, the entry $P'_{m,s}(t)$ is specified by [6], [7]

$$P'_{m,s}(t) = \left\{\begin{array}{ccl} P_{m,s}(t) & : & \text{User } r \xrightarrow{=1} \text{User } m \\ 0 & : & \text{User } r \xrightarrow{=0} \text{User } m \end{array}\right. . \qquad (12)$$

The column $[M(s-1)+m]$ of the parity matrix $\boldsymbol{P}$ shown in Fig. 1 contains the set of parity coefficients valid for the s^{th} PF transmitted by User m during the cooperative phase $[M(s-1)+m]$. Hence, the entire column $P'_{m,s}(t)$, $\forall t = [1, 2, ..., k_1 M]$ will be set to zeros, if the BS could not successfully receive the s^{th} PF:

$$P'_{m,s}(t) = 0, \forall t = [1, 2, ..., k_1 M] : \text{User } m \xrightarrow{s^{th}\text{PF}=0} \text{BS}. \quad (13)$$

C. Detection model

As the system proceeds through an actual transmission session, the corresponding modified transfer matrix $\boldsymbol{G}'$ consisting of its identity matrix $\boldsymbol{I}'$ and its parity matrix $\boldsymbol{P}'$ is formed, where $\boldsymbol{I}'$ is generated from (9), while $\boldsymbol{P}'$ is determined in turn by (11), (12) and (13). The frames successfully received at the BS can be represented as

$$(a)\ \boldsymbol{X}\boldsymbol{I}' = \boldsymbol{Y}_{I'},\ (b)\ \boldsymbol{X}\boldsymbol{P}' = \boldsymbol{Y}_{P'}, \quad (14)$$

where $\boldsymbol{X} = \{I_1(1), I_2(2), ..., I_M(k_1 M)\}$ is a matrix representing the IFs transmitted by the M users during the transmission session of the system, while the matrices of $\boldsymbol{Y}_{I'}$ and $\boldsymbol{Y}_{P'}$ represent the frames successfully received at the BS during the broadcast phases and cooperative phases, respectively. In line with [6], [7], we assume that the BS is aware of how each PF was constructed, hence $\boldsymbol{G}'$ is known at the BS. Since the matrix $\boldsymbol{I}'$ may be different from $\boldsymbol{I}$, the BS can certainly recover a set $\boldsymbol{X}_{I'}$ of IFs, which is a subset of $\boldsymbol{X}$, from $\boldsymbol{Y}_{I'}$ according to:

$$\boldsymbol{X}_{I'} = \boldsymbol{Y}_{I'}. \quad (15)$$

Substituting $\boldsymbol{X}_{I'}$ given by (15) into (14b) we have

$$\left(\boldsymbol{X} - \boldsymbol{X}_{I'}\right)\boldsymbol{P}' = \boldsymbol{Y}_{P'} - \boldsymbol{X}_{I'}\boldsymbol{P}'. \quad (16)$$

Then, a set $\tilde{\boldsymbol{X}}_{P'}$ of IFs is retrieved from (16) by using the Gaussian elimination algorithm [18]. Ultimately, the entire set of IFs recovered at the BS is $\tilde{\boldsymbol{X}}_{P'} \bigcup \boldsymbol{X}_{I'}$ out of the $\boldsymbol{X}$ of IFs.

Having presented the detection model above, let us now characterise the system's optimistic performance estimated by the PRBM employed in [6] by recalling the example detailed in (6) and (7). According to the prediction of the PRBM, the BS can recover Rank$(\boldsymbol{G}'_{2\times4}) = 1$ IF, where $\boldsymbol{G}'_{2\times4}$ is given in (8). However, in fact the BS cannot recover any IF, because we cannot determine two IFs, i.e. both $I_1(1)$ and $I_2(2)$, from a single equation, which is inferred from (15) and (16) as $1 \times I_1(1) + 2 \times I_2(2)$.

III. Design and Analysis

A. Near-Capacity Code Design

According to (1), (3) and (5), the average SNR_r per frame can be expressed as

$$SNR_r = \frac{\mathrm{E}[|h_s|^2]\mathrm{E}[|h_f|^2]\mathrm{E}[|x|^2]}{N_0} = \frac{|h_s|^2}{N_0}, \quad (17)$$

where we have $\mathrm{E}[|x|^2] = 1$ and $\mathrm{E}[|h_f|^2] = 1$ for uncorrelated Rayleigh fading channels and $\mathrm{E}[|h_s|^2] = |h_s|^2$ for quasi-static Rayleigh fading channels. Given a specific SNR_r, we can generate the EXIT chart [12] of the channel coding scheme for transmission over the uncorrelated Rayleigh fading channel.

As stated in Section I, a near-capacity IrCC-URC-MPSK channel coding scheme is chosen for the sake of approaching the achievable channel capacity. For the sake of brevity and readability, we present the IrCC-URC-Quadrature Phase Shift Keying (IrCC-URC-QPSK) design procedure using our generically applicable EXIT-chart aided method, which is briefly summarised as follows:

Step1: Create the EXIT curve of the inner decoder constituted by our URC-QPSK scheme for different SNR_r values;

Step2: We opt for the data rate $R = \eta R_c = 1$, we fix the IrCC code rate $R_c = 0.5$ and employ the EXIT curve matching algorithm of [10] for generating the optimised weighting coefficients $\alpha_i, i = 1, ..., 17$, of the 17 different-rate component IrCC codes. More specifically, we opt for the set of codes facilitating decoding convergence to a vanishingly low BER at the lowest possible SNR_r, while ensuring that the Monte-Carlo simulation based decoding trajectory reaches the point of (1,1) at the top-right corner of the corresponding EXIT chart. This implies that a near-capacity performance can be achieved, as detailed in [15].

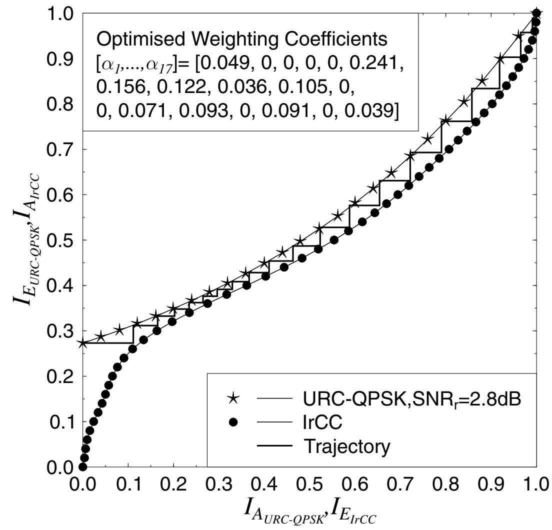

Fig. 2. The EXIT curves of the inner decoder URC-QPSK and the outer decoder IrCC for a single transmission link along with the Monte-Carlo simulation based decoding trajectory.

Having implemented the design steps mentioned above, we obtain the EXIT curves and the corresponding IrCC component-code weighting coefficients α_i, $i = 1, ..., 17$, as shown in Fig. 2. Again as detailed in [15], these weighting coefficients α_i determine the particular fraction of the input stream to be encoded by the i^{th} IrCC component code having a code rate of α_i. The EXIT-chart results show that provided $J = 20$ iterations were affordable, the trajectory would reach the $(1, 1)$ point in Fig. 2, which guarantees a vanishingly low BER.

Furthermore, the area property of EXIT-charts [19] states that the area under the EXIT curve of an inner decoder component is approximately equal to the attainable channel capacity, provided that the channel's input symbols are equiprobable. Hence we exploited the area property of EXIT-charts [19] to determine the achievable DCMC capacities of the URC-QPSK and IrCC-URC-QPSK systems, which are quantified in Fig. 3. It is seen in Fig. 3 that the capacity of the URC-QPSK scheme almost coincides with the DCMC-QPSK curve. The numerical results of Fig. 3 also show the attainable channel capacity improvements corresponding to J = 1,10,20 and 40 iterations. There is only a negligible further improvement for having $J = 40$ in comparison to $J = 20$. It is also demonstrated in Fig. 3 that the IrCC-URC-QPSK scheme's capacity curve is only about $(2.8 - 1.8) = 1.0$dB away from DCMC-QPSK capacity curve for $J = 20$.

Our simulation results seen in Fig. 4 verify the accuracy of our EXIT chart analysis. When employing $J = 20$ iterations between the IrCC and URC components, our IrCC-URC-QPSK channel coding scheme has a vanishingly low BER for SNRs in excess of 2.8dB, provided that the transmission frame length is sufficiently high. At this stage we also define the relaying-aided reduced-distance-related pathloss-reduction. Naturally, this pathloss-reduction becomes unity for each direct source-to-destination link [20]. We also observe from

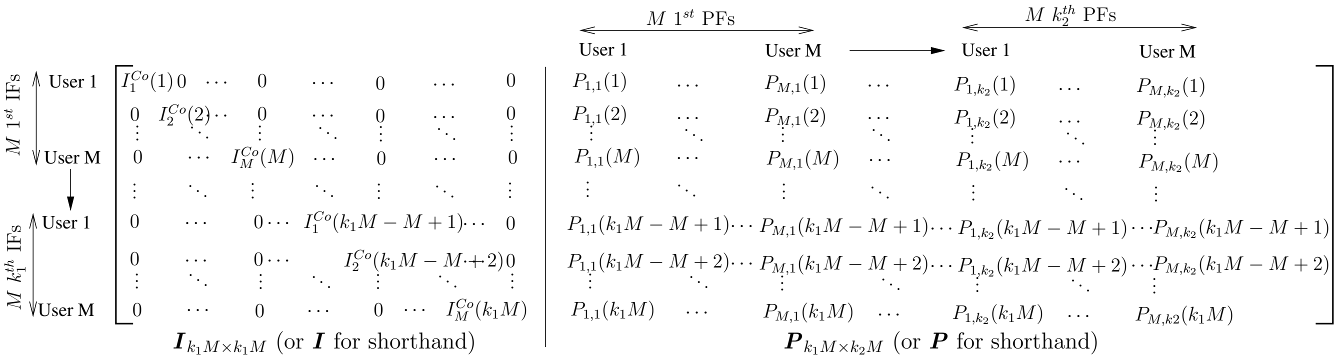

Fig. 1. The transfer matrix $\boldsymbol{G}_{k_1M \times k_1M + k_2M}$ [6], [7] illustrating a transmission session of the system having M users transmitting in $(k_1M + k_2M)$ phases.

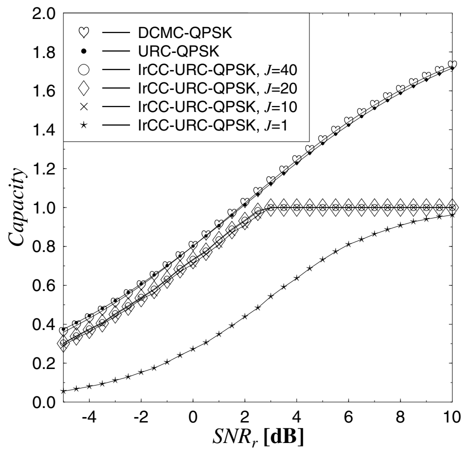

Fig. 3. Channel capacity comparison for the QPSK, URC-QPSK and IrCC-URC-QPSK based systems.

Fig. 4 that as expected, a shorter frame length results in an improved FER performance, hence to strike a compromise, we opted for a frame size of 10^4 symbols for our system.

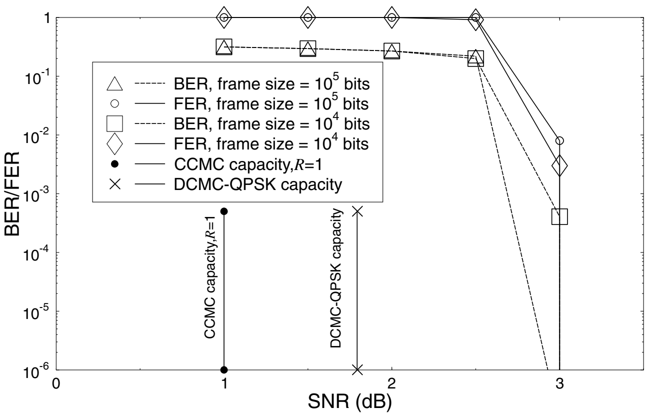

Fig. 4. Performance of the proposed IrCC-URC-QPSK scheme under uncorrelated Rayleigh fading conditions.

B. Network Coding Design

In line with [6], [7], we assume that all the links in Near-Capacity Multi-user Network-coding (NCMN) based system are supported by channels having the same data rate R. For notational convenience, we characterise our proposed NCMN based system by using the set of parameters $(R, M, k_1, k_2, \boldsymbol{G}, R_{info}, D_{NCMN})$, where the system's overall data rate R_{info} is expressed as [6], [7]

$$R_{info} = \frac{k_1}{k_1 + k_2}, \quad (18)$$

while the diversity order D of the system is bounded [6], [7]:

$$M + k_2 \le D_{NCMN} \le Mk_2 + 1. \quad (19)$$

By observing the R_{info} expression of (18) and the D_{NCMN} formula of (19), it is plausible that we may conceive different systems having the same rate R_{NCMN}, but different diversity order D_{NCMN} by independently adjusting k_1, k_2 and M. In other words, using (18) and (19), we are able to design a network-coding based system having the highest possible diversity order at a given overall system data rate of R_{NCMN}. A higher diversity order implies that the system is capable of achieving an improved FER performance.

In order to demonstrate the design principles mentioned above, let us consider a $\boldsymbol{G}_{2\times4}$-based system and a $\boldsymbol{G}_{4\times8}$-based system. The matrix $\boldsymbol{G}_{2\times4}$ is given in (6), and $\boldsymbol{G}_{4\times8}$ is obtained from a systematic generator matrix of a Reed-Solomon code as [6], [7]:

$$\boldsymbol{G}_{4\times8} = \begin{bmatrix} 1 & 0 & 0 & 0 & | & 3 & 7 & 3 & 6 \\ 0 & 1 & 0 & 0 & | & 5 & 7 & 7 & 4 \\ 0 & 0 & 1 & 0 & | & 2 & 4 & 6 & 1 \\ 0 & 0 & 0 & 1 & | & 5 & 5 & 3 & 2 \end{bmatrix}. \quad (20)$$

The $\boldsymbol{G}_{2\times4}$-based system is represented by $(R = 0.5, M = 2, k_1 = 1, k_2 = 1, \boldsymbol{G}_{2\times4}, R_{info} = 0.5, 3 \le D_{(2\times4)NCMN} \le 3)$, and the $\boldsymbol{G}_{4\times8}$-based system is characterised by $(R = 0.5, M = 2, k_1 = 2, k_2 = 2, \boldsymbol{G}_{4\times8}, R_{info} = 0.5, 4 \le D_{(4\times8)NCMN} \le 5)$. The two systems are comparable, since they both have the same R, M and R_{info} values. However, the more complex transfer matrix $\boldsymbol{G}_{4\times8}$ has a higher diversity order of $4 \le D_{(4\times8)NCMN} \le 5$ (as opposed to $3 \le D_{(2\times4)NCMN} \le 3$). This also means that the $\boldsymbol{G}_{4\times8}$-based system is expected to have a superior FER performance in comparison to the $\boldsymbol{G}_{2\times4}$-based system.

IV. Simulation Results and Discussions

The FER versus SNR performance of the $\boldsymbol{G}_{2\times4}$ and $\boldsymbol{G}_{4\times8}$ based systems employing the IrCC-URC-Binary Phase Shift Keying (IrCC-URC-BPSK) scheme [15] and the idealised/perfect CCMC and DCMC channel coding schemes is shown in Fig. 5. We use the IrCC-URC-BPSK coding scheme having a data rate $R = 1 \times 0.5 = 0.5$, in order to facilitate a comparison between our results and the previous results presented in [6], [7]. The IrCC-URC-BPSK coding scheme was also designed by the same procedure as that used for the IrCC-URC-QPSK, as detailed in Section III-A [15].

It can be seen from Fig. 5 and Fig. 6 that the difference in the diversity order of the $\boldsymbol{G}_{2\times4}$ and $\boldsymbol{G}_{4\times8}$ based systems, as specified in Section III-B, is reflected by the different slope of the performance curves. As a benefit, the $G_{4\times8}$-based system outperforms the $G_{2\times4}$-based system by about from 4.2 dB to 4.4 dB at an FER of 10^{-4} in the cases of using the CCMC, DCMC, IrCC-URC-BPSK and IrCC-URC-QPSK channel coding schemes.

Another important result gleaned from both Fig. 5 and Fig. 6 is that the performance of the NCMN systems using the idealised/perfect CCMC and DCMC channel coding schemes represents the best-case performance bound of all NCMN systems using realistic channel coding schemes, provided that the equivalent data rates R of those schemes are the same.

Fig. 5 and Fig. 6 substantiates our analysis provided in Section II-C, where the performance estimate found with the aid of the PRBM was always superior but optimistic in comparison to that obtained by the actual simulations. More explicitly, it is shown in Fig. 5 and Fig. 6 that their deviation was found to be from 0.3 dB to 0.5 dB at an FER of 10^{-4}.

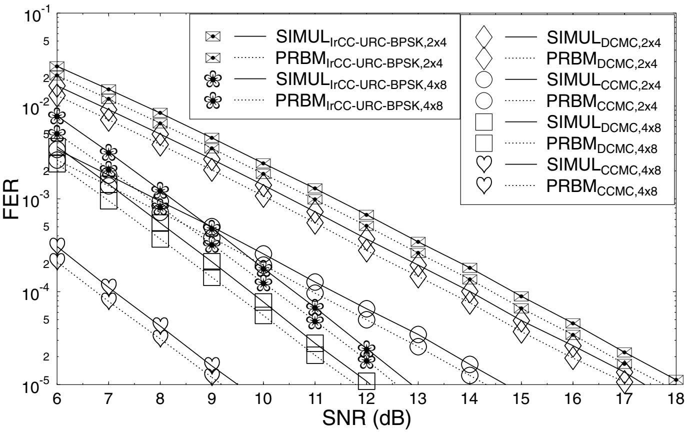

Fig. 5. FER versus SNR performance of the $G_{2\times4}$ and $G_{4\times8}$ based systems employing the realistic channel coding scheme IrCC-URC-BPSK and idealised/perfect CCMC and DCMC channel coding schemes.

As seen in Fig. 5 and Fig. 6, the performance of the $G_{4\times8}$ and $G_{2\times4}$-based systems using our IrCC-URC-BPSK(QPSK) scheme was within 0.7 dB to 0.8 dB at an FER of 10^{-4} from that of the corresponding systems relying on the assumption of using an idealised/perfect DCMC channel coding scheme.

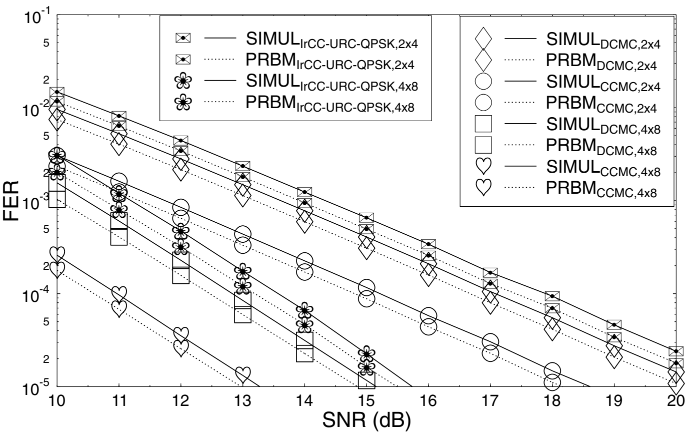

Fig. 6. FER performance comparison between $G_{2\times4}$ and $G_{4\times8}$ based systems employing the realistic channel coding scheme IrCC-URC-QPSK and idealised/perfect CCMC and DCMC channel coding schemes.

V. Conclusions

In this contribution, we investigated new Near-Capacity Multi-user Network-coding based systems using our IrCC-URC-MPSK channel coding scheme, which was designed with the aid of EXIT charts. The achievable performance was benchmarked against the corresponding systems employing the idealised/perfect channel coding schemes operating exactly at the CCMC and DCMC capacities.

References

[1] R. Ahlswede, N. Cai, S.-Y. Li, and R. Yeung, "Network information flow," *Information Theory, IEEE Transactions on*, vol. 46, pp. 1204 – 1216, jul 2000.

[2] A. Asterjadhi, E. Fasolo, M. Rossi, J. Widmer, and M. Zorzi, "Toward network coding-based protocols for data broadcasting in wireless ad hoc networks," *IEEE Transactions on Wireless Communications*, vol. 9, pp. 662 –673, Feb. 2010.

[3] M. Xiao and T. Aulin, "Optimal decoding and performance analysis of a noisy channel network with network coding," *IEEE Transactions on Communications*, vol. 57, pp. 1402 –1412, may 2009.

[4] T. Ho, M. Medard, R. Koetter, D. Karger, M. Effros, J. Shi, and B. Leong, "A random linear network coding approach to multicast," *IEEE Transactions on Information Theory*, vol. 52, pp. 4413 –4430, Oct. 2006.

[5] M. Jafari, L. Keller, C. Fragouli, and K. Argyraki, "Compressed network coding vectors," in *2009 IEEE International Symposium on Information Theory (ISIT 2009)*, pp. 109 –113, June-July 2009.

[6] J. L. Rebelatto, B. F. Uchôa-Filho, Y. Li, and B. Vucetic, "Generalized distributed network coding based on nonbinary linear block codes for multi-user cooperative communications," in *2010 IEEE International Symposium on Information Theory (ISIT 2010)*, pp. 943 –947, June 2010.

[7] J. L. Rebelatto, B. F. Uchôa-Filho, Y. Li, and B. Vucetic, "Multi-user cooperative diversity through network coding based on classical coding theory," *Submitted to IEEE Transactions on Signal Processing*, [Online]. Available: http://arxiv.org/abs/1004.2757.

[8] M. Xiao and M. Skoglund, "Multiple-user cooperative communications based on linear network coding," *IEEE Transactions on Communications*, Dec. 2010.

[9] M. Xiao and M. Skoglund, "M-user cooperative wireless communications based on nonbinary network codes," in *IEEE Information Theory Workshop on Networking and Information Theory, 2009. (ITW 2009)*, pp. 316 –320, June 2009.

[10] M.Tücher and J. Hagenauer, "Exit charts of irregular codes," in *Proceeding of the 36th Annual Conference on Information Sciences and Systems [CDROM], (Princeton, NJ, USA)*, March 2002.

[11] M. Tuchler, "Design of serially concatenated systems depending on the block length," *IEEE Transactions on Communications*, vol. 52, pp. 209–218, Feb. 2004.

[12] S. ten Brink, "Convergence behavior of iteratively decoded parallel concatenated codes," *IEEE Transactions on Communications*, vol. 49, pp. 1727–1737, Oct. 2001.

[13] S. X. Ng, J. Wang, M. Tao, L.-L. Yang, and L. Hanzo, "Iteratively decoded variable length space-time coded modulation: Code construction and convergence analysis," *IEEE Transactions on Wireless Communications*, vol. 6, pp. 1953–1963, May 2007.

[14] R. Tee, R. G. Maunder, and L. Hanzo, "Exit-chart aided near-capacity irregular bit-interleaved coded modulation design," *IEEE Transactions on Wireless Communications*, vol. 8, pp. 32–37, Jan. 2009.

[15] L. Hanzo, O.Alamri, M. E.Hajjar and N.Wu, *Near-Capacity Muti-Functional MIMO Systems*. New York, USA : John Wiley and Sons, 2009.

[16] D. Tse and P. Viswanath, *Fundamentals of Wireless Communications*. Englewood Cliffs, NJ, USA: Cambridge: Cambridge University Press, 2005.

[17] S. X. Ng and L. Hanzo, "On the MIMO channel capacity of multidimensional signal sets," *IEEE Transactions on Vehicular Technology*, vol. 55, pp. 528 – 536, March 2006.

[18] C. F. Golub, Gene H.; Van Loan, *Matrix Computations*. Johns Hopkins Studies in Mathematical Sciences: Johns Hopkins University Press, 1996.

[19] A. Ashikhmin, G. Kramer, and S. ten Brink, "Extrinsic information transfer functions: model and erasure channel properties," *IEEE Transactions on Information Theory*, vol. 50, pp. 2657–2673, Nov. 2004.

[20] H. Ochiai, P. Mitran, and V. Tarokh, "Design and analysis of collaborative diversity protocols for wireless sensor networks," in *Proc. VTC2004-Fall Vehicular Technology Conference 2004 IEEE 60th*, vol. 7, pp. 4645–4649, Sept. 26–29, 2004.